Cavity-Assisted Single-Mode and Two-Mode Spin-Squeezed States via Phase-Locked Atom-Photon Coupling

Yong-Chang Zhang,[1,2] Xiang-Fa Zhou,[1,2,*] Xingxiang Zhou,[1,2] Guang-Can Guo,[1,2] and Zheng-Wei Zhou[1,2,†]
[1]Key Laboratory of Quantum Information, Chinese Academy of Sciences, University of Science and Technology of China, Hefei 230026, China
[2]Synergetic Innovation Center of Quantum Information and Quantum Physics, University of Science and Technology of China, Hefei 230026, China
(Received 30 August 2016; published 24 February 2017)

We propose a scheme to realize the two-axis countertwisting spin-squeezing Hamiltonian inside an optical cavity with the aid of phase-locked atom-photon coupling. By careful analysis and extensive simulation, we demonstrate that our scheme is robust against dissipation caused by cavity loss and atomic spontaneous emission, and it can achieve significantly higher squeezing than one-axis twisting. We further show how our idea can be extended to generate two-mode spin-squeezed states in two coupled cavities. Because of its easy implementation and high tunability, our scheme is experimentally realizable with current technologies.

DOI: 10.1103/PhysRevLett.118.083604

Introduction.—Since the early work of Kitagawa and Ueda [1] and others [2,3], spin-squeezed states have attracted much interest due to their close relations with quantum information processing [4–9] and precision metrology [1,2,10–12]. In the original work of Kitagawa and Ueda [1], two mechanisms, namely, one-axis twisting (OAT) and two-axis countertwisting (TACT), were proposed to generate spin-squeezed states. Preparation of such novel states has been the subject of many studies in various physical setups, such as feedback systems [13], Bose-Einstein condensates (BECs) [8,12,14–21], Rydberg lattice clocks [22], and atomic systems in cavities [23–29]. To the best of our knowledge, all experiments to date have focused on OAT spin squeezing, whereas TACT spin-squeezed states have not yet been realized in experiments.

In quantum metrology, it is theoretically demonstrated [1,2] that TACT states are fundamentally superior to OAT states because measurement systems based on them can approach the Heisenberg limit in which the precision of the measurement scales with $1/N$, with N being the number of particles in the system. By contrast, the precision allowed by OAT states scales with $1/N^{2/3}$. Hence, it remains a very important task to generate and exploit TACT spin-squeezed states using methods and techniques within the reach of current technologies. There have been a few theoretical proposals, such as converting OAT into effective TACT [17–19], implementing TACT with molecular states [6,20], utilizing ultracold atoms in two cavities [28], employing feedback in the measurement system [13], and using toroidal BECs [21]. Nevertheless, because of the demanding experimental requirements of these schemes, it remains experimentally challenging to generate TACT spin-squeezed states.

In this Letter, we propose a scheme to realize a TACT Hamiltonian in a cavity-atom system. Our proposal relies on phase-locked coupling between atoms and photons only. Since both the atoms and the cavity modes are only virtually excited, it has the important advantage of being largely immune to atomic and cavity dissipation. Furthermore, our scheme can be easily generalized to generate two-mode spin-squeezed (TMSS) states by coupling two cavities, which can be used to estimate two observables simultaneously even when they do not commute. They are widely used in many quantum applications, such as entanglement demonstration [30,31], quantum teleportation [32], and quantum metrology [33]. Considering the rapid advances in cavity technology, including the availability of high-finesse optical cavities and strong cavity-atom coupling [34–40], our proposal can be realized with no fundamental difficulty.

Effective Hamiltonian.—We start by considering an ensemble of N four-level atoms in an optical cavity coupled to a single cavity mode and external laser fields. The explicit level configuration is illustrated in Fig. 1, where g_1 and g_2 are the cavity-atom coupling strengths driving the atomic transitions $|1\rangle \leftrightarrow |3\rangle$ and $|2\rangle \leftrightarrow |4\rangle$ and $\tilde{\Omega}_{1,2}$ and $\Omega_{1,2}$ are Rabi frequencies of the external laser fields, and $\Delta_{1,2}$, $\delta_{1,2}$, and $\gamma_{1,2}$ are detunings. To realize the desired

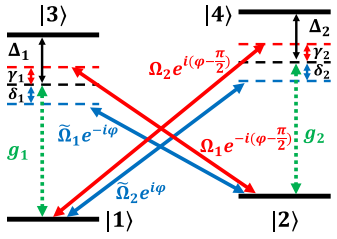

FIG. 1. Atomic energy levels and transitions between them. The complex Rabi frequencies $\tilde{\Omega}_1 e^{-i\varphi}$, $\tilde{\Omega}_2 e^{i\varphi}$, $\Omega_1 e^{-i[\varphi-(\pi/2)]}$, and $\Omega_2 e^{i[\varphi-(\pi/2)]}$ are associated with four phase-locked driving lasers. $g_{1,2}$ is the coupling strength between the atom and the cavity mode. $\Delta_{1,2}$, $\delta_{1,2}$, and $\gamma_{1,2}$ are detunings.

 © 2017 American Physical Society

TACT interaction, we also assume a fixed relative phase of $\pi/2$ $(-\pi/2)$ between Ω_1 (Ω_2) and $\tilde{\Omega}_1$ $(\tilde{\Omega}_2)$ [41,42]. The Hamiltonian reads

$$H=\sum_{j=1}^{N}\Big\{\frac{e^{i\varphi}}{2}[\tilde{\Omega}_2 e^{-i(\Delta_2+\delta_2)t}-i\Omega_2 e^{-i(\Delta_2-\gamma_2)t}]|1\rangle_j\langle 4| + \frac{e^{-i\varphi}}{2}[\tilde{\Omega}_1 e^{-i(\Delta_1+\delta_1)t}+i\Omega_1 e^{-i(\Delta_1-\gamma_1)t}]|2\rangle_j\langle 3| + g_1|1\rangle_j\langle 3|a^\dagger e^{-i\Delta_1 t}+g_2|2\rangle_j\langle 4|a^\dagger e^{-i\Delta_2 t}+\text{H.c.}\Big\}, \quad (1)$$

where $a^\dagger$ (a) is the creation (annihilation) operator of the cavity mode, $\pm\varphi$ and $\pm[\varphi-(\pi/2)]$ are the phases of the external laser fields, and the detunings are defined as $\Delta_{1(2)}=\omega_{3(4)}-\omega_{1(2)}-\omega_c$, $\gamma_{1(2)}=\omega_{2(1)}-\omega_{1(2)}-\omega_c+\omega_{L_1(L_2)}$, and $\delta_{1(2)}=\omega_{1(2)}-\omega_{2(1)}+\omega_c-\omega_{\tilde{L}_1(\tilde{L}_2)}$, with $\omega_{L_{1,2}},\omega_{\tilde{L}_{1,2}}$ and ω_c being the frequencies of the driving lasers and the cavity mode. The rotating wave approximation was used to derive the Hamiltonian in Eq. (1) in the rotating frame defined by $H_0=\sum_{j=1}^{N}\sum_{k=1}^{4}\omega_k|k\rangle_j\langle k|+\omega_c(a^\dagger a+\frac{1}{2})$. To simplify our discussion, here and in the following, we assume $\delta=\delta_1=\delta_2$, $\gamma=\gamma_1=\gamma_2$, and set $\varphi=0$. For large detunings with

$$|\Delta_{1,2}|,|\Delta_{1,2}+\delta|,|\Delta_{1,2}-\gamma|\gg|g_{1,2}|,|\Omega_{1,2}|,|\tilde{\Omega}_{1,2}|, \quad (2)$$

all of the high energy levels can be adiabatically eliminated, leading to the following effective Hamiltonian involving only the two lowest states and the cavity mode:

$$H'=\{c_z-c_z'\sin[(\delta+\gamma)t]\}S_z - \Big[\frac{A}{2}S_x a^\dagger e^{i\delta t}+\frac{B}{2}S_y a^\dagger e^{-i\gamma t}+\text{H.c.}\Big]. \quad (3)$$

Here, the collective atomic spin operators are defined as $S_z=\frac{1}{2}\sum_{j=1}^{N}(|1\rangle_j\langle 1|-|2\rangle_j\langle 2|)$, $S_x=\frac{1}{2}\sum_{j=1}^{N}(|1\rangle_j\langle 2|+|2\rangle_j\langle 1|)$, and $S_y=\frac{i}{2}\sum_{j=1}^{N}(|2\rangle_j\langle 1|-|1\rangle_j\langle 2|)$. The explicit expressions for the coefficients c_z, c_z', A, and B can be found in the Supplemental Material [43].

If we further assume that the effective couplings in Eq. (3) are much weaker than the detunings, i.e.,

$$|\delta|,|\gamma|,|\delta\pm\gamma|\gg N|A|/4,\qquad N|B|/4, \quad (4)$$

the cavity mode is virtually excited only and can be adiabatically eliminated, too. We then obtain the following effective Hamiltonian:

$$H_{\text{eff}}=c_z S_z-c_x S_x^2+c_y S_y^2, \quad (5)$$

with $c_x=(A^2/4\delta)$ and $c_y=(B^2/4\gamma)$ [43]. This is the celebrated Lipkin-Meshkov-Glick (LMG) model [2]. When $c_z=0$ and $c_x=c_y=\chi$, it reduces to the standard TACT Hamiltonian in Ref. [1]. Experimentally, all coefficients $c_{x,y,z}$ can be controlled by adjusting the Rabi frequencies of the driving lasers. If necessary, c_z can also be compensated for by an external magnetic field [47].

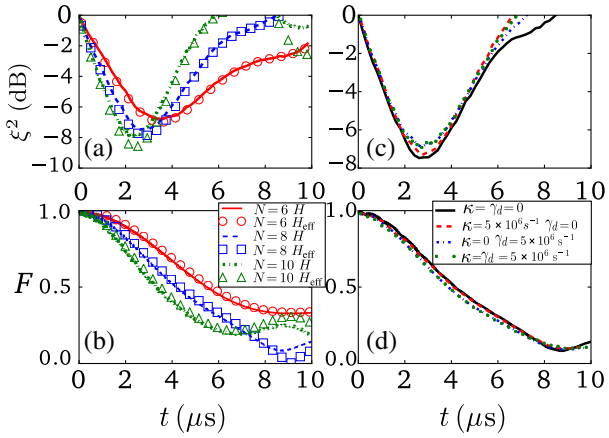

FIG. 2. (a), (b) Time evolution of ξ^2 and F with H in Eq. (1) and H_{eff} in Eq. (5) without dissipation for $N=6$, 8, and 10. (c), (d) Time evolution of ξ^2 and F under the original Hamiltonian H in Eq. (1) with dissipation for $N=8$.

To characterize the degree of spin squeezing, we introduce the parameter [1,2]

$$\xi^2=\frac{(\Delta S_\perp)^2_{\text{min}}}{S/2}. \quad (6)$$

Here, $S=N/2$, with $\mathbf{S}=(S_x,S_y,S_z)$ being the total spin operator, and $(\Delta S_\perp)^2_{\text{min}}=(\langle\mathbf{S}_\perp^2\rangle-\langle\mathbf{S}_\perp\rangle^2)_{\text{min}}$ is the minimum spin fluctuation in the direction perpendicular to the average spin $\langle\mathbf{S}\rangle$. A state is a spin coherent state (spin-squeezed state) if $\xi^2=1$ $(\xi^2<1)$ [1].

Numerical simulation.—In order to check the validity of our approximations, we numerically simulate the system evolution under the effective Hamiltonian in Eq. (5) and the original Hamiltonian in Eq. (1) and compare the results. To fulfill the approximations, the explicit parameters are chosen as follows: $g_{1,2}=\Omega_{1,2}=\tilde{\Omega}_{1,2}=\Omega=5\times10^7\,\text{s}^{-1}$, $\Delta_{1,2}=\Delta=10^9\,\text{s}^{-1}$, $\delta_{1,2}=10^8\,\text{s}^{-1}$, and $\gamma_{1,2}=1.26\times10^8\,\text{s}^{-1}$. With these parameters, the effective model reduces to a standard TACT Hamiltonian with $c_z=0$ and $\chi=5.69\times10^4\,\text{s}^{-1}$. We also assume that, initially, the cavity is in the vacuum state and the atoms are all in the state $|1\rangle$, which corresponds to a coherent spin state in the z direction. Shown in Figs. 2(a) and 2(b) are the time dependences of the squeezing parameter ξ^2 and the overlap function $F=|\langle\psi(0)|\psi(t)\rangle|$, with the initial state of the system in the ideal case without cavity leakage $(\kappa=0)$ and atomic spontaneous decay $(\gamma_d=0)$. The state evolution dictated by the effective TACT Hamiltonian in Eq. (5) agrees very well with that calculated directly from the original full Hamiltonian in Eq. (1), strong evidence that all approximations employed in our derivation are reasonable.

We note in Fig. 3(b) that, although the maximum achievable squeezing (i.e., the minimum ξ^2) increases with the number of atoms N [2,17], the time the squeezing takes to reach its maximum increases with N, too. This is because the nonlinear squeezing coefficients $c_x(c_y)$ in Eq. (5) must decrease with N in order to maintain the virtual excitation of the system as dictated by Eq. (4). Though virtual excitation reduces the influence of the dissipation, its eventual effect on squeezing must be carefully evaluated because of the longer squeezing time required to reach the optimal squeezing. For this purpose, we numerically solve the master equation [26,48,49] of the system

$$\frac{\partial\rho}{\partial t} = -i[H,\rho] - \frac{\kappa}{2}\mathcal{D}(a,\rho) - \frac{1}{2}\sum_{k=1}^{N}\sum_{s=1}^{4}\gamma_{ks}\mathcal{D}(L_{ks},\rho). \quad (7)$$

Here, $\mathcal{D}(O,\rho) = O^\dagger O\rho + \rho O^\dagger O - 2O\rho O^\dagger$, ρ is the density matrix, κ and γ_{ks} are the cavity loss rate and the atomic spontaneous decay rate, and $L_{k1} = |1\rangle_k\langle 3|$, $L_{k2} = |2\rangle_k\langle 3|$, $L_{k3} = |1\rangle_k\langle 4|$, and $L_{k4} = |2\rangle_k\langle 4|$ are the jump operators. The results are shown in Figs. 2(c) and 2(d) for $N = 8$. It is seen that the squeezing is robust against dissipation and the maximum achievable squeezing is only slightly influenced by cavity loss and atomic spontaneous emission as strong as $\kappa = \gamma_d = 5\times 10^6$ s^{-1}. Since we have confirmed the validity of the virtual excitation of the cavity mode in earlier simulations, we can adiabatically eliminate the cavity field from the full master equation to increase the scale of our simulated system. This results in the following master equation [26] that involves only the atomic spin degrees of freedom:

$$\frac{\partial\rho_{\rm eff}}{\partial t} = -i[H_{\rm eff},\rho_{\rm eff}] - \frac{\gamma_d}{2}\sum_{\alpha=z,\pm}\sum_{k=1}^{N} a_\alpha\mathcal{D}(\sigma_\alpha^k,\rho_{\rm eff}) - \frac{\kappa}{2}\left(\frac{A^2}{4\delta^2}\mathcal{D}(S_x,\rho_{\rm eff}) + \frac{B^2}{4\gamma^2}\mathcal{D}(S_y,\rho_{\rm eff})\right), \quad (8)$$

where $\sigma_z^k = |1\rangle_k\langle 1| - |2\rangle_k\langle 2|$, $\sigma_+^k = |1\rangle_k\langle 2|$, $\sigma_-^k = |2\rangle_k\langle 1|$, and the explicit expressions for $a_{z,\pm}$ can be found in the Supplemental Material [43]. Using Eq. (8), we can numerically simulate larger systems with more atoms. In Fig. 3(a), we plot the maximum achievable squeezing in our system with strong dissipation, as well as the maximum squeezing attainable in an ideal OAT Hamiltonian with no dissipation. The results show that, even in the presence of strong dissipation, our system can achieve a higher degree of squeezing than what is possible with ideal OAT, and the advantage grows with the size of the system. In Fig. 3(b), we compare the maximum achievable squeezing of an ideal TACT Hamiltonian in Eq. (5) ($c_z = 0$) with that of ideal OAT for larger system sizes on the order of 10^3–10^5. A large advantage is observed with our scheme. For a system size of $N = 10^5$ atoms, as in recent experiments [29,50],

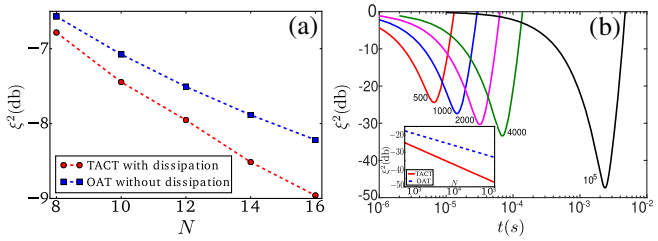

FIG. 3. (a) Comparison of the maximum achievable squeezing in our system with strong atomic and cavity dissipation rates $\kappa = \gamma_d = 5\times 10^6$ s^{-1} and in a dissipation-free OAT system $H_{\rm OAT} = \chi S_x^2$. Other parameters are the same as in Fig. 2, except that $\Omega = 2\times 10^7$ s^{-1}. (b) Time evolution of ξ^2 in our system with $N = 10^3$–10^5 atoms and no dissipation. (Inset) The maximum achievable squeezing in our system and in OAT, both without dissipation. The relevant parameters are $\Delta_1 = -\Delta_2 = 1.88\times 10^{10}$ s^{-1}, $\gamma = 2\delta = 1.26\times 10^{10}$ s^{-1}, and $A = B/\sqrt{2} = 0.4\delta/N$, where $N = 500$, 1000, 2000, 4000, and 10^5.

the ideal Hamiltonian equation (5) for our system can reach a squeezing of −47.4 dB, significantly higher than current schemes based on OAT [8,11,12,14,27] with the same system size. Since the atomic decay time, estimated as $1/\gamma_{\rm eff}$, with $\gamma_{\rm eff}\sim(\Omega^2/4\Delta^2)\gamma_d \approx (\gamma\chi/g^2)\gamma_d$ [23,25,27], can be longer than the time required to reach the optimal squeezing, $t_o = 1.58\ln N/(3N\chi)$ [17]—e.g., when $N = 10^5$—using the parameters in Fig. 3(b) with $g = 1.26\times 10^7$ s^{-1} and $\gamma_d = 3.77\times 10^7$ s^{-1}, the atomic decay time $1/\gamma_{\rm eff}\approx 13$ ms is larger than $t_o(10^5)\approx 2.4$ ms, and the influence of cavity loss is much weaker than that of the atoms' decay, as illustrated in Fig. 2(c), a high degree of squeezing can be achieved.

Two-mode spin-squeezed states.—Our scheme can be extended to generate TMSS states [30,31,51] using two cavities. Assuming a coupling between the two cavity modes, we have the following total Hamiltonian in the rotating frame:

$$H_{\rm tc} = H_L + H_R - \tilde{J}(a_L^\dagger a_R e^{i\Delta\omega t} + \text{H.c.}), \quad (9)$$

where $a_{L,R}^\dagger(a_{L,R})$ is the creation (annihilation) operator for the left and right cavity mode, $\tilde{J}$ is the tunneling rate between the cavities, and $\Delta\omega = \omega_c^L - \omega_c^R$ is the detuning between the two cavities with the local Hamiltonian $H_{\alpha\in(L,R)} = -(A_\alpha/2)S_x^\alpha a_\alpha^\dagger e^{i\delta_\alpha t} - (B_\alpha/2)S_y^\alpha a_\alpha^\dagger e^{-i\gamma_\alpha t} + \text{H.c.}$ When the coefficients and detunings satisfy the following conditions,

$$\delta_L = -\delta_R = \delta > 0, \quad -\gamma_L = \gamma_R = \gamma > 0$$
$$\Delta\omega = \delta + \gamma, \quad A_L = A_R = A, \quad B_L = B_R = B, \quad (10)$$

the effective Hamiltonian for the two-cavity system can then be written [43]

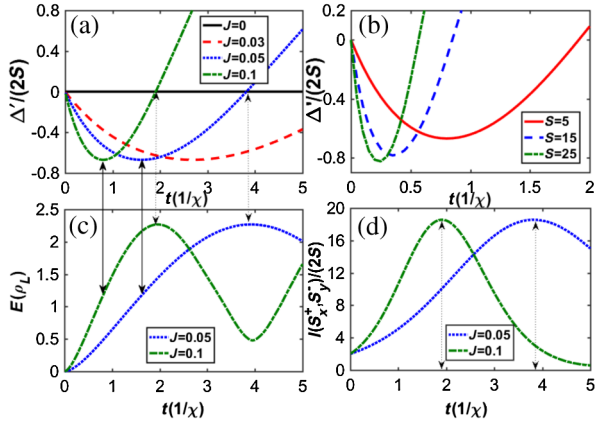

FIG. 4. Time evolution of squeezing, entanglement, and quantum Fisher information of two-mode spin-squeezed states with the same total spin number for the two modes. (a) Δ' vs t while $S = N/2 = 5$, and $J = 0$, 0.03, 0.05, 0.1. (b) Δ' vs t while $J = 0.1$, and $S = 5$, 15, 25. (c) Dependence of the von Neumann entropy $E(\rho_L)$ on time for $J = 0.05$, 0.1 when $S = 5$. (d) The quantum Fisher information for $|\Psi(t)\rangle$ at $J = 0.05$, 0.1 when $S = 5$.

$$H_T = \chi[(S_z^L)^2 - (S_z^R)^2] + 2J\chi(S_x^L S_y^R + S_y^L S_x^R), \qquad (11)$$

with $\chi = (A^2/4\delta) = (B^2/4\gamma)$, and $J = (\tilde{J}/\sqrt{\delta\gamma})$. The second term in H_T gives rise to a TMSS state. The first term, which describes the on-site nonlinear interaction in each cavity, has no contribution when $S_z^L = S_z^R$.

A TMSS state can be identified by checking to see that it satisfies the inequality $\Delta' = (\Delta S_x^{(-)})^2 + (\Delta S_y^{(+)})^2 - \langle S_z^{(+)}\rangle < 0$, with $S_k^{(\pm)} = S_k^L \pm S_k^R$ $(k = x, y, z)$ [30,31,51]. This criterion implies that fluctuations in nonlocal observables S_x^- and S_y^+ can be suppressed at the same time. Thus, it is possible to achieve higher measurement precisions for them simultaneously. When the total spins inside the two cavities are equal, $S_L = S_R$, a TMSS state can be obtained by letting the system evolve under H_T from an initial state in which both cavities are in a coherent state: $|\Psi(0)\rangle = |S, S\rangle$, with $|m_i^L, m_j^R\rangle$ $(m_i^{L,R} = -S, -S+1, \ldots, S-1, S)$ being the eigenvectors of S_z, and $S = N/2$ the total spin. Plotted in Figs. 4(a) and 4(b) is the time evolution of $\Delta'(t)$. One can see that Δ' is always zero when $J = 0$, as both cavities are decoupled in this case. When there is photon tunneling between the cavities—and thus $J \neq 0$—Δ' can become negative, which signals the emergence of TMSS states. Comparing Fig. 4(a) with Fig. 4(b), we note that the time it takes to reach $\Delta'_{\min}$, the minimum value of Δ', is controlled by the coupling strength J, and $\Delta'_{\min}$ decreases as S increases. To investigate the entanglement of the TMSS state, we have further calculated the von Neumann entropy $E(\rho_L) = -\rho_L \ln \rho_L$ of the reduced density matrix $\rho_L = Tr_R(|\Psi\rangle\langle\Psi|)$, as well as the two-parameter quantum Fisher information $I(S_x^+, S_y^-)_{ij} = 2\langle\Psi|\{H_i, H_j\}|\Psi\rangle - 4\langle\Psi|H_i|\Psi\rangle\langle\Psi|H_j|\Psi\rangle$ [52], with $(i, j) = (1, 2)$. Here, $H_{1(2)} = S_x^+(S_y^-)$, and $\{*, *\}$ is the anticommutation relation. The results are shown in Figs. 4(c) and 4(d). The TMSS state generated by the effective Hamiltonian (11) leads to $I(S_x^+, S_y^-)_{11} = I(S_x^+, S_y^-)_{22} = I(S_x^+, S_y^-)$ [see Fig. 4(d)] and $I(S_x^+, S_y^-)_{12,21} = 0$. Comparing Figs. 4(c) and 4(d) with Fig. 4(a), we find that Δ' reaches its minimum (marked by black solid arrows) when $E(\rho_L) = E(\rho_L)_{\max}/2$. This result implies that the TMSS state at $\Delta'_{\min}$ is not a maximum entangled state. In addition, both $I(S_x^+, S_y^-)$ and $E(\rho_L)$ attain their maxima only when Δ' evolves back to zero.

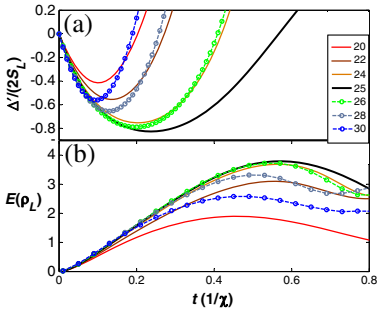

FIG. 5. Time evolution of squeezing and entanglement of two-mode spin-squeezed states with different total spin numbers for the two modes. (a) Δ' and (b) $E(\rho_L)$ vs t for a fixed $S_L = N_L/2 = 25$ and $J = 0.1$. S_R varies from 20 to 30.

To explore the influence of the imbalance between S_L and S_R on the TMSS state, we fix S_L and vary S_R with the initial state $|S_L, S_R\rangle$. In Fig. 5, the numerical result shows that $\Delta'_{\min}$ reaches the optimal value only when $S_L = S_R$ and increases as $\Delta S = |S_L - S_R|$ increases. The time it takes to reach $\Delta'_{\min}$, t_o also decreases with ΔS. In contrast to the balanced case, $E(\rho_L)$ at t_o is smaller than $E(\rho_L)_{\max}/2$, and it does not reach the maximum when Δ' evolves back to zero, as shown in Fig. 5(b). Therefore, to obtain a TMSS state with a lower Δ', it is helpful to prepare two cavities with equal total spins.

Experimental consideration.—Experimentally, our model can be realized with an ensemble of ^{87}Rb atoms in optical cavities [25,26]. Two hyperfine states $|F = 1, m_F = 1\rangle$ and $|F = 2, m_F = 2\rangle$ of the manifold $5S_{1/2}$ can be used as the lower energy states $|1\rangle$ and $|2\rangle$ in Fig. 1. Their energy splitting is 4.27×10^{10} s^{-1}. Two other hyperfine states of the manifold $5P_{1/2}$ with a splitting of 5.03×10^9 s^{-1} can be selected as the higher excited states $|3\rangle$ and $|4\rangle$. This choice leads to a detuning of $\Delta_1 - \Delta_2 = 3.77 \times 10^{10}$ s^{-1}. To implement the effective TACT Hamiltonian in Eq. (5) with $c_z = 0$ and $c_x = c_y$, we have a total of ten adjustable parameters, namely, $\Delta_{1,2}$, $\Omega_{1,2}$, $\tilde{\Omega}_{1,2}$, $\delta_{1,2}$, and $\gamma_{1,2}$. They need to satisfy the constraints $\Delta_1 - \Delta_2 = 3.77 \times 10^{10}$ s^{-1}, $(A^2/\delta) = (B^2/\gamma)$, and several others listed in the Supplemental Material [43]. Since the number of these constraints is less than the number of adjustable parameters, both the TACT model and the LMG model can be achieved by adjusting the detunings and couplings.

Conclusion.—We proposed a scheme to realize an effective TACT Hamiltonian in a cavity-atom interacting system via phase-locked atom-photon coupling. We proved that the approximations used in our derivation are justified and demonstrated that greater degrees of squeezing can be achieved in our system than existing schemes based on OAT. Furthermore, we generalized our ideas to a two-cavity system and showed how TMSS states can be realized. Because of the high tunability of our scheme, it is possible to access the full parameter ranges of the LMG model, enabling us to explore its rich physics [53–58].

Y.-C. Z. thanks Jun-Kang Chen for the kind help on the numerical simulation. This work was funded by the National Plan on Key Basic Research and Development (Grant No. 2016YFA0301700), the National Natural Science Foundation of China (Grants No. 11574294, No. 61490711, and No. 11474266), the Major Research plan of the NSFC (Grant No. 91536219), and the "Strategic Priority Research Program (B)" of the Chinese Academy of Sciences (Grant No. XDB01030200).

*xfzhou@ustc.edu.cn
†zwzhou@ustc.edu.cn

[1] M. Kitagawa and M. Ueda, Phys. Rev. A **47**, 5138 (1993).
[2] J. Ma, X. Wang, C. P. Sun, and F. Nori, Phys. Rep. **509**, 89 (2011).
[3] D. J. Wineland, J. J. Bollinger, W. M. Itano, F. L. Moore, and D. J. Heinzen, Phys. Rev. A **46**, R6797 (1992).
[4] B. Julsgaard, J. Sherson, J. Ignacio Cirac, and J. Fiurášek, and E. S. Polzik, Nature (London) **432**, 482 (2004).
[5] K. Hammerer and A. S. Sørensen, and E. S. Polzik, Rev. Mod. Phys. **82**, 1041 (2010).
[6] K. Helmerson and L. You, Phys. Rev. Lett. **87**, 170402 (2001).
[7] A. Micheli, D. Jaksch, J. I. Cirac, and P. Zoller, Phys. Rev. A **67**, 013607 (2003).
[8] M. F. Riedel, P. Böhi, Y. Li, T. W. Hänsch, A. Sinatra, and P. Treutlein, Nature (London) **464**, 1170 (2010).
[9] T. E. Lee, F. Reiter, and N. Moiseyev, Phys. Rev. Lett. **113**, 250401 (2014).
[10] W. Muessel, H. Strobel, D. Linnemann, D. B. Hume, and M. K. Oberthaler, Phys. Rev. Lett. **113**, 103004 (2014).
[11] B. Lücke, M. Scherer, J. Kruse, and L. Pezzé, F. Deuretzbacher, P. Hyllus, O. Topic, J. Peise, W. Ertmer, J. Arlt, L. Santos, A. Smerzi, and C. Klempt, Science **334**, 773 (2011).
[12] C. Gross, T. Zibold, E. Nicklas, and J. Estève, and M. K. Oberthaler, Nature (London) **464**, 1165 (2010).
[13] L. K. Thomsen, S. Mancini, and H. M. Wiseman, J. Phys. B **35**, 4937 (2002).
[14] J. Estève, C. Gross, A. Weller, S. Giovanazzi, and M. K. Oberthaler, Nature (London) **455**, 1216 (2008).
[15] M. J. Martin, M. Bishof, M. D. Swallows, X. Zhang, C. Benko, J. von-Stecher, A. V. Gorshkov, A. M. Rey, and Jun Ye, Science **341**, 632 (2013).
[16] J. Lian, L. Yu, J.-Q. Liang, G. Chen, and S. Jia, Sci. Rep. **3**, 3166 (2013).
[17] Y. C. Liu, Z. F. Xu, G. R. Jin, and L. You, Phys. Rev. Lett. **107**, 013601 (2011).
[18] J. Y. Zhang, X. F. Zhou, G. C. Guo, and Z. W. Zhou, Phys. Rev. A **90**, 013604 (2014).
[19] W. Huang, Y.-L. Zhang, C.-L. Zou, X.-B. Zou, and G.-C. Guo, Phys. Rev. A **91**, 043642 (2015).
[20] M. Zhang, K. Helmerson, and L. You, Phys. Rev. A **68**, 043622 (2003).
[21] T. Opatrný, M. Kolář, and K. K. Das, Phys. Rev. A **91**, 053612 (2015).
[22] L. I. R. Gil, R. Mukherjee, E. M. Bridge, M. P. A. Jones, and T. Pohl, Phys. Rev. Lett. **112**, 103601 (2014).
[23] F. Dimer, B. Estienne, A. S. Parkins, and H. J. Carmichael, Phys. Rev. A **75**, 013804 (2007).
[24] A. E. B. Nielsen and K. Mølmer, Phys. Rev. A **77**, 063811 (2008).
[25] S.-B. Zheng, Phys. Rev. A **86**, 013828 (2012).
[26] E. G. Dalla Torre, J. Otterbach, E. Demler, V. Vuletic, and M. D. Lukin, Phys. Rev. Lett. **110**, 120402 (2013).
[27] L. Yu, J. Fan, S. Zhu, G. Chen, S. Jia, and F. Nori, Phys. Rev. A **89**, 023838 (2014).
[28] L. Yu, C. Li, J. Fan, G. Chen, T.-C. Zhang, and S. Jia, Chin. Phys. B **25**, 050301 (2016).
[29] M. H. Schleier-Smith, I. D. Leroux, and V. Vuletić, Phys. Rev. Lett. **104**, 073604 (2010).
[30] B. Julsgaard, A. Kozhekin, and E. S. Polzik, Nature (London) **413**, 400 (2001).
[31] D. W. Berry and B. C. Sanders, J. Phys. A **38**, L205 (2005).
[32] D. W. Berry and B. C. Sanders, New J. Phys. **4**, 8 (2002).
[33] C. Vaneph, T. Tufarelli, and M. G. Genoni, Quantum Meas. Quantum Metrol. **1**, 12 (2013).
[34] D. K. Armani, T. J. Kippenberg, S. M. Spillane, and K. J. Vahala, Nature (London) **421**, 925 (2003).
[35] S. M. Spillane, T. J. Kippenberg, K. J. Vahala, K. W. Goh, E. Wilcut, and H. J. Kimble, Phys. Rev. A **71**, 013817 (2005).
[36] T. Aoki, B. Dayan, E. Wilcut, W. P. Bowen, A. S. Parkins, T. J. Kippenberg, K. J. Vahala, and H. J. Kimble, Nature (London) **443**, 671 (2006).
[37] F. Brennecke, T. Donner, S. Ritter, T. Bourdel, M. Köhl, and T. Esslinger, Nature (London) **450**, 268 (2007).
[38] Y. Colombe, T. Steinmetz, G. Dubois, F. Linke, D. Hunger, and J. Reichel, Nature (London) **450**, 272 (2007).
[39] K. W. Murch, K. L. Moore, S. Gupta, and D. M. Stamper-Kurn, Nat. Phys. **4**, 561 (2008).
[40] H. Ritsch, P. Domokos, F. Brennecke, and T. Esslinger, Rev. Mod. Phys. **85**, 553 (2013).
[41] J. Cho, D. G. Angelakis, and S. Bose, Phys. Rev. Lett. **101**, 246809 (2008).
[42] Z.-X. Chen, Z.-W. Zhou, X. Zhou, X.-F. Zhou, and G.-C. Guo, Phys. Rev. A **81**, 022303 (2010).
[43] See Supplemental Material at http://link.aps.org/supplemental/10.1103/PhysRevLett.118.083604, which includes Refs. [26,44–46], for the detailed derivations of Eq. (5), Eq. (8), and Eq. (11).
[44] D. F. V. James and J. Jerke, Can. J. Phys. **85**, 625 (2007).
[45] T. F. Roque and A. Vidiella-Barranco, J. Opt. Soc. Am. B **31**, 1232 (2014).

[46] Y.-C. Liu, Y.-F. Xiao, X. Luan, Q. Gong, and C. W. Wong, Phys. Rev. A **91**, 033818 (2015).
[47] L.-M. Duan, E. Demler, and M. D. Lukin, Phys. Rev. Lett. **91**, 090402 (2003).
[48] M. B. Plenio and P. L. Knight, Rev. Mod. Phys. **70**, 101 (1998).
[49] D. G. Norris, A. D. Cimmarusti, L. A. Orozco, P. Barberis-Blostein, and H. J. Carmichael, Phys. Rev. A **86**, 053816 (2012).
[50] O. Hosten, N. J. Engelsen, R. Krishnakumar, and M. A. Kasevich, Nature (London) **529**, 505 (2016).
[51] M. G. Raymer, A. C. Funk, B. C. Sanders, and H. de Guise, Phys. Rev. A **67**, 052104 (2003).
[52] J. Liu, X.-X. Jing, and X. Wang, Sci. Rep. **5**, 8565 (2015).
[53] O. Castaños, R. López-Peña, J. G. Hirsch, and E. López-Moreno, Phys. Rev. B **74**, 104118 (2006).
[54] F. de los Santos, E. Romera, and O. Castaños, Phys. Rev. A **91**, 043409 (2015).
[55] M. A. Caprio, P. Cejnar, and F. Iachello, Ann. Phys. (N.Y.) **323**, 1106 (2008).
[56] Z.-G. Yuan, P. Zhang, S.-S. Li, J. Jing, and L.-B. Kong, Phys. Rev. A **85**, 044102 (2012).
[57] G. Engelhardt, V. M. Bastidas, W. Kopylov, and T. Brandes, Phys. Rev. A **91**, 013631 (2015).
[58] P. Ribeiro, J. Vidal, and R. Mosseri, Phys. Rev. E **78**, 021106 (2008).